EFFECTIVE CUTTING AND SURFACE CONTENT IN INCONEL 718 SUPERALLOY FINISH The Effects of Different Lubrication and Cooling Conditions on Face Milling

Dr G Raja Kumar [1], Perumallapalli Gandhi [2], Dr. B. Ravi [3]

Assistant Professor [1,2,3]

Department of Mechanical engineering,

[1,3] Swarna Bharati Institute of Science and Technology, Khammam, TS-507002

[2] SV engineering college, Surya Peta (DIST). TS-508213

ABSTRACT:

Inconel718, a nickel-based superalloy, with legendary thermal and mechanical capabilities. Inconel is a challenging material to deal with because of the high temperatures generated during its production. It cuts significantly more cleanly and efficiently with proper cooling and lubrication (CL) techniques. Here, we'll take a look at the four possible cutting techniques for Inconel 718 and see how they stack up: CMQLC, dry cutting, flood cutting, and cryogenic cutting. Cutting pressures, temperatures, tool wear, chip dimensions, Ra, microstructure, and RS are among the many factors that are tracked. The results show that processing is improved when CL is included. When compared to DC, CMQLC often yields cooler outcomes. While all four approaches reduced tool chipping area and surface Ra by 25% and 32.05%, respectively, CMQLC was the least effective. The subsurface influence depth increased by 10.2%, the TRS by 7.9%, and the MCRS by 3.9% when the RS was taken into account. It is also possible to get a superior RS condition during machining when the mechanical thermal ratio is large. The CMQLC has a beneficial effect on cutting performance, workpiece surface integrity, and pollution levels in the environment.

Relevant terms include Inconel 718, cooling and lubrication (CL), surface integrity, and cutting performance.

1. **INTRODUCTION**

Due to its low thermal conductivity, corrosion resistance, and anti-fatigue characteristics, nconel 718 nickel-based superalloy finds extensive usage in nuclear reactors, aircraft engine turbine discs and blades, and several other industries. Inconel 718 is one of the hardest materials to cut due to its exceptional qualities. Poor surface integrity, limited tool life, and high coolant consumption are some of the cutting characteristics of Inconel 718. Inconel 718 machining remains a formidable obstacle, despite considerable advancements in tools and cooling and lubrication (CL) schemes. A considerable increase in temperature occurs at the cutting region because almost all of the energy is transformed into heat during the cutting process. By reducing friction and efficiently cooling the cutting zone, coolant is a better alternative to blocking heat production.2

Typically, the surface that has been machined is tensile residual stress (TRS). The addition of CL has the potential to improve the hardness and decrease the surface roughness, which in turn may raise the compressive resistance stress (CRS), decrease the TRS, and ultimately increase the fatigue life of the components.4 Research on Inconel 718 for surface integrity prediction has shown a robust relationship between RS, fatigue life, and roughness.Therefore, it is important to

investigate how CL circumstances affect Inconel 718 cutting performance and surface integrity.

Cryogenic gas and lubricant oil are delivered concurrently by CMQL, a technique that lowers the cutting coolant cost.6 With its excellent cutting capability and surface roughness, the CMQL has recently found widespread usage in cutting Ti6Al4V,7 AISI 316L,8 and AISI 10459. Lubricants that have a high friction coefficient but a low viscosity may increase tool life by as much as 200%.11 In addition, the CMQLC makes short work of chip removal by reducing both thickness and friction.12 It is debatable whether microscopic droplets can efficiently reach the cutting region due to the high temperatures produced by Inconel 718 cutting. Grinding Inconel 718 with CMQL improves surface integrity compared to conventional cutting methods.13 CMQL's advantage in turning Inconel 718 is confirmed by analysing microstructure, surface roughness, cutting forces, tool wear, and surface roughness.16 Even if it's more eco-friendly and can attain over 90% FC, the lubricating effect isn't up to par with emulsion oil.17 The use of high-pressure coolant improves cutting performance while decreasing tool wear and adhesion chip wear.18 Cryogenic coolants increase tool life compared to FC and MQL at room temperature by 57% and 20%, respectively. Thus, the CMQLC may achieve a balance between technology and the environment by replacing the old technique of cooling and lubricating.19,20

Tool wear and RS have been the primary foci of CL cutting studies on Inconel 718. Surface3,21 and modelling have been the primary areas of study about the RS that results after cutting.22,23 dollars Research on Inconel 718's cutting performance and surface integrity has been conducted, but there has been a dearth of thorough evaluations of either, particularly with regard to the RS at subsurface.25 As a result, Inconel 718 milling under DC, FC, CC, and CMQLC conditions is the subject of this study. We analyse the chips and measure the cutting forces and temperature.

Measurements of surface roughness, microstructure, and RS reveal the surface integrity.

2. Experimental setup

Workpiece properties

In this experiment, Inconel 718 that has been heat treated (;HV 452) is used. This data is derived from the following sources: elemental and metallographic examination, tensile testing of the experimental materials.26 Additionally, Table 1 displays the primary chemical components. Figure 1(a) shows the microstructure of Inconel 718, which consists of the following phases: d, g#, g##, and NbC. After heat treatment, Inconel 718's stress-strain curve is shown in Figure 1(b). At 20°C, the yield stress s0.2 is 1308.6 MPa.

Experimental procedure

The DX6080 is used to conduct the milling experiment. The workpiece's finished surface, which has a border size of 18 mm x 30 mm. Cemented carbide covered with AlTiN serves as the substrate for the VSM-4E(D4) tool from ZCC.CT (Figure 2(b)).

Figure 2(a)–(c) displays the experimental setup. The refrigeration and oil mist modules, which are the major components of CMQL equipment (PMPM15-S, SUNAIR, Figure 2(a)), have their own volume and inject oil continuously. Cryogenic air (measurement value: 23°C) is expelled from the vortex nozzle while high-pressure gas (4-8 bar) is introduced into the system via the pipeline. The nozzle is used to spray the oil mist, which is a pulse-regulated mist (0.05-0.2 L/h) made of lubricant6 that is based on vegetable oil. Table 2 shows the tool-recommended range of cutting parameters; use these values as a guide for selecting intermediate values.

Cutting forces are reduced, chips are shorted and removed, friction and

scratches are reduced, and cutting becomes easier with high-pressure cryogenic flow. Compressed gas is primarily used for cooling in this system, while oil mist is used for lubricating.27 The cutting area is prepared by pouring FC with cutting fluid; DC does not impose any CL procedures. In Figure 2(a) and (d), you can see the milling model that is helped by CMQL. Examining the cutting performance and surface integrity is done by marking a lengthy and stable cutting region on the workpiece in blue.

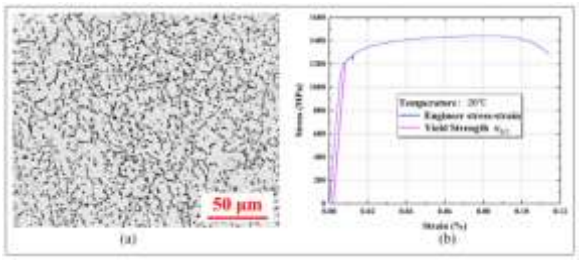

Figure 1. Microstructure and tensile properties of the Inconel 718 superalloy: (a) OM microstructure and (b) tensile stress-strain curve.

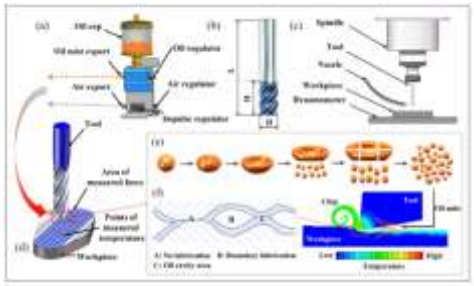

Figure 2. Experimental setup, milling, and lubrication models: (a) CMQL device (PMPM15-S), (b) tool model (VSM-4E), (c) the milling model, (d) experimental model, (e) breakage of oil droplets, and (f) lubrication model.

3. RESULTS AND DISCUSSION

Lubrication mechanism

According to the theory of liquid sprays28 and fluid dynamics,29 the CMQL lubrication model and the oil droplet breaking model are obtained. The breakage of oil droplets is shown in Figure 2(e). The essence of lubricant atomization is that under the external force of droplets, droplets break up and separate. In this process, external forces (such as nozzle extrusion pressure) are constantly competing with the surface tension and

Table 2. The cutting parameters.

Cutting speed (r/min)	Feed rate (mm/min)	Axial depth (mm)	Radial depth (mm)
1800	500	0.20	0.50

viscosity of droplets. Because the surface tension allows making the droplets to maintain a simple spherical, the surface energy of the whole droplets is minimized; and

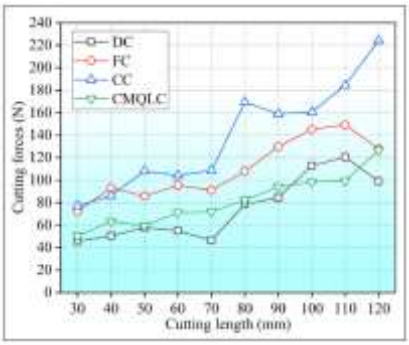

Figure 3. The variation of cutting force with the CL condition.

the viscosity of oil droplets prevents the deformation of liquid. When the external force of droplets is bigger than the surface tension and viscosity of the liquid, droplets will separate.

Figure 2(f) shows the CMQL lubricating mechanism. This means that when the nozzle sprays droplets, the surface of the droplets will experience a vibration wave caused by the gas vibrations close to the jet path, which will progressively intensify. Subsequently, the droplets will fragment into many smaller ones, as well as flake liquid and lengthy droplets. Factors such as nozzle structure, jet state, and environmental variables dictate the size. Subsequently, the droplets undergo a process of breaking and atomisation, whereby they undergo various forms of crushing as a result of the high-speed airflow. The ellipsoid, cumuliform, and

semi-bubble shapes of the droplets are all affected by environmental factors including gas pressure. When the jet's velocity exceeds the threshold, the semi-bubble droplets' tops start to crack, resulting in annular liquid bands. The annular liquid bands may hold 70% of the mass of the full oil droplets before injection since their volume is proportional to the size of the droplets before breaking. The droplets undergo further crushing as they are propelled by the high-speed jet. Those outside the jet are broken up into flakes, while those in the centre are shattered into many microbubbles. Ultimately, every single droplet is reduced to microdroplets smaller than 2 mm.

Lubrication effect of oil is directly proportional to its volume, according to the principle of the boundary lubrication film generated by coolant between two contact surfaces. Therefore, the quantity of oil mist injected greatly affects the film's creation. There is no lubrication (A), border lubrication (B), or oil cavity region (C) in the cutting area, as illustrated in Figure 2(f).

Additionally, the CMQL processes far less oil mist than the coolant. Furthermore, droplets are prevented from accessing the contact region by the high temperatures and pressures at the tool. Thus, boundary lubrication is the most common kind of liquid friction between the tool-chip and tool-workpiece interfaces, and it is difficult to provide total liquid friction between these surfaces. During metal cutting, large droplets transform into the paste, which then adheres to both the tool and the workpiece. Water evaporates more quickly from the contact zone and is better able to reach the cutting zone when droplets are smaller.9 Therefore, little oil droplets may improve surface wettability by lowering the cutting force and friction coefficient.30 Boosting the pressure of atomised air improves the wetting area, which in turn increases the ability to dissipate heat. So, it's clear that reducing residual stress works.31 Oil droplets of a smaller size are therefore better for cutting.

Cutting forces

A Kistler dynamometer (9257B), together with an A/D data acquisition board, charge amplifier, data collector, and acquisition software (DynoWare), make up the cutting forces measuring system.

Figure 3 shows how the average cutting force changes as a function of cutting length. There is a dramatic rise in cutting forces at 80 mm. Despite a huge fluctuation range, DC cutting forces are quite minimal since hardness decreases considerably at high temperatures. Cutting forces are more intense and are rather consistent in FC. The cutting forces are the most significant and unpredictable under CC because of the high levels of friction and tool wear. While both CMQLC and DC forces are quite tiny, the trend for CMQLC is more consistent. This is due to the fact that CMQLC offers superior lubrication, which helps to minimise friction in the cutting region. The CMQLC's cutting forces are so minimal and steady.

Cutting temperature

I use a portable infrared thermometer (testo 868) to check the cutting temperature. With reliable cutting, six measurement spots are chosen (Figure 2).

Both the average and the fluctuation in temperature are shown in Figure 4(a) and 4(b), respectively. While both the tool and CL have an impact on the cutting temperature, all four CL approaches exhibited an upward trend in the temperatures measured. While FC and CMQLC show a minor rise, DC and CC see a significant increase. Since CL is not supplied, DC has the highest amplitude. While CC does a good job of cooling the cutting region, it does very little to mitigate frictional heat. More vibration and severe tool wear are the results of using larger cutting forces. The CMQL provides oil mist, which effectively reduces friction, and further reduces tool wear. The heat is taken away by the

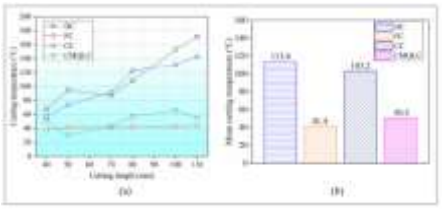

Figure 4. Cutting temperature variation with CL condition (a) and its average value (b).

coolant in a short time in FC. Whereas, due to the defects of the non-contact measurement itself, the actual cutting temperature may be higher than theirs. And the FC still has the best cooling effect and provides water lubrication; the cutting temperature under CMQL is also acceptable, so it is necessary to add lubri-cating medium in the cutting of high hardness materials such as Inconel 718.

Cutting edge chipping

The microscope (EASSON-EVM2515T) is used to examine the tool's wear.

Important parameters influencing surface integrity include tool wear and chipping, which decrease the clearance angle, increase the contact area between the tool and workpiece, and elevate temperatures and forces. The shift in the subsurface is mostly driven by the enormous stress that they induce. Materials used in the work piece will undergo plastic deformation and expansion as a result of the high temperature.32

Figure 5(a) displays the tool's flank topography and end face. You can see the matching chipped region in Figure 5(b). There is a lot of wear and tear on the tool's flank and cutting edge, and the chipping area reaches 0.19 mm2 due to the high temperature and increased friction between contact pairs in DC. By lubricating the contact pairs, the coolant in FC decreases friction, eliminates cutting heat, and chips the material. An area of just 0.12 mm2 is affected by chipping.

The cryogenic gas pre-cools the contact pairs, and the highest chipping is recorded in CC, reaching 0.26 mm2. The tool's brittleness may rise somewhat, and the workpiece's surface hardens. Contact pairs experience high levels of immediate friction and impact force due to the lack of lubrication, leading to edge chipping. Forces, temperature, and surface roughness all have a role in the succeeding cutting, which severely damages the tool and leads to worse surface quality. Consistent with findings in Bagherzadeh et al.7, cutting materials with high hardness, such Inconel 718, need lubrication in addition to cooling.

There is less resistance and friction between the contact pairs thanks to the CMQLC. Area of chipping is 0.09 mm2. The oil, however, will cling to a few surface flaws, leading to wear and tear. Finally, CMQLC causes the least amount of flank chipping, which means the tools last the longest.

Surface roughness

To identify the surface morphologies acquired by cutting with the same parameters, the ALICONA company's 3D profile scanner InfmiteFocus G4g is used. To get the surface cloud map and determine the Ra, a sample length of 4 mm was used.

Figure 6 displays the surface characterisation. The amount of wear and tear on the surfaces of DC and CC varies with respect to their topographies. There is a clear groove that backs up the idea that the surface is poor in CC due to severe wear and scratches. Perhaps due to the tool's severe damage, the Ra of CC is the greatest, reaching 3.397. Surface damage is more severe due to high temperature and large friction, even if DC has a lower Ra. Another issue is that not all chips are ejected promptly. The surface topography of FC is relatively flat, without

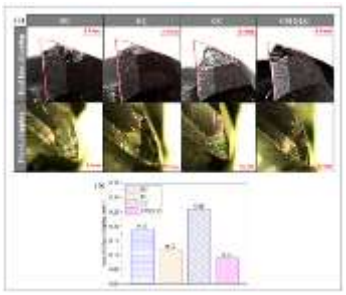

Figure 5. Tool chipping under different CL conditions: (a) topography of edge chipping and (b) areas of flank chipping.

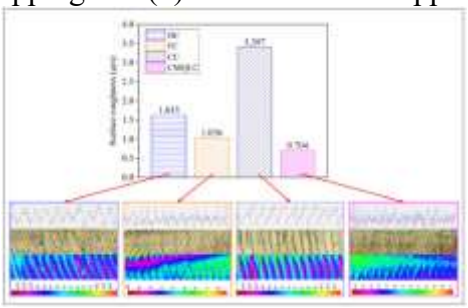

Figure 6. Surface roughness and morphology under different CL conditions.

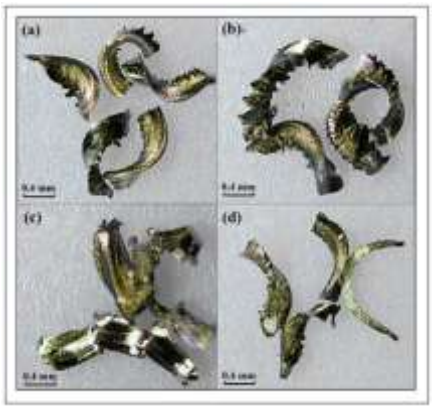

Figure 7. Chip morphology under different CL conditions:
(a) DC, (b) FC, (c) CC, and (d) CMQLC

scratches, and with less wear. Compared to DC (Ra 1.633) and FC (Ra 1.036), the CMQLC obtains rela- tively minimal surface roughness (Ra 0.704) due to its excellent CL effects. The surface profile generated by CMQLC may be messy because the tiny chips are adhered to the surface by oil, but CMQLC is still considered to be the best way.

Chip morphology

Microscopy also reveals the chip morphology. Heat generation and dissipation determine the cutting area temperature. Improving the material removal rate is advantageous, and the heat dissipation capacity of the chip determines the dominating position of mechanical load and thermal impact for machining deformation. Therefore, surface integrity is highly affected by chip shape.33

The chip morphologies are shown in Figure 7. Chips made with DC have serrated edges and are more homogeneous in size. The shear plane becomes a sheer body and the shear angle decreases as a result of rising pressure in the shear zone; this is the method by which a serrated edge is formed. Axial shear happens in the direction of the fractures that form on the free surface when the material approaches its strain limit. Serrated chips are formed when fractures and adiabatic shear work together. As coolant is poured over the chip, it takes on a spiral pattern, with the curving degree reduced, length slightly raised, and serrated edge heightened.

This may be because the lower tem- perature is not enough to make the chip produce large bending, so the chip length is longer when the chip

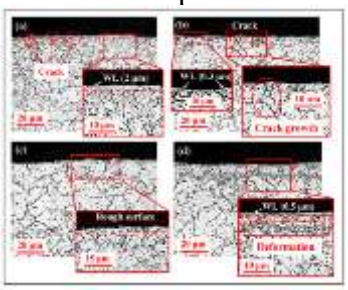

Figure 8. The metallographic structure under different CL conditions: (a) DC, (b) FC, (c) CC, and (d) CMQLC.

breaks. When using the cryogenic method, the chip no longer presents regular morphology but appears extru- sion chip with fewer or no serrated edges. The chip brit- tleness increases at low temperatures, and it is easier to break. Nevertheless, the cutting edge of the tool with large wear is blunt, and the chips are mainly caused by extrusion and cracking. When the CMQL method is adopted, the chip is narrow, the

curling degree is small, and the edge sawtooth is not obvious. The chip-breaking performance is good at low temperatures, the friction force under oil mist lubrication is small, and the squeezing effect is weakened. This type of chip facil- itates material removal and reduces surface damage.

Microstructure

To analyse the subsurface metallographic structure, the sample surface is mechanically ground and polished, and the microstructure is studied with a metallographic microscope (Leica DM2700 M) and scanning electron microscope (ZEISS EVO 18).

According to Pusavec et al.4, when the cutting strength is minimal, the fibre structure does not undergo any notable changes. Grain plastic deformation is mostly associated with tool wear and cutting force, whereas the mechanical effect is the dominant factor in cryogenic cutting.34 Cutting pressures are higher and granular plastic deformation is more noticeable as tool wear becomes more severe. One potential negative aspect of surface integrity is the processing-induced white layer (WL).35 Figure 8 displays the metallographic microstructure. The WL (2 mm) appears under the DC, which means that WL is more likely to form at higher temperatures and worn tools; small cracks appeared on the surface, some grain crushing appeared on the subsurface, and

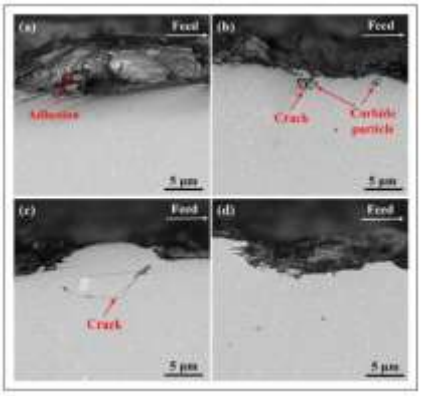

Figure 9. The metallographic structure under different CL conditions: (a) DC, (b) FC, (c) CC, and (d) CMQLC.

the plastic deformation layer (PDL) is not apparent, it is more like a layer of dynamically recovery microstruc- ture. WL decreased to about 0.3 mm in FC, but cracks appeared on the surface and extended deeper into the interior. Under CC, because the tool is seriously dam-aged, the cutting process is irregular, the damaged sur- face is rough and the surface integrity is worse, and the microstructure shows no obvious cutting characteristics. There are few surface cracks under CMQLC, and the WL is about 0.5 mm deep; obvious plastic deformation occurs in the subsurface grains, and the depth of the PDL is about 13 mm, it is more like dynamically recrys- tallized microstructure. This is because the mechanical effect is more dominant, and grain plastic deformation is mainly related to tool wear and cutting force.34 The depth of the WL can be significantly reduced by using coolant, and the PDL can be obtained by using CMQL, which helps to improve fatigue life.

The SEM images of the cross-section of the work- piece after processing are shown in Figure 9. In DC, the adhesion phenomenon occurs. This is due to the material affinity becoming larger under high tempera- tures, and cold welding occurs, so the material adheres to the surface of the workpiece. The use of FC reduces the phenomenon of adhesion, but cracks appear at hard particles. Under CC, due to the chipping of the tool and the absence of a lubricating medium, a large mechanical load is generated, so cracks appear on the subsurface and have a tendency to expand. With CMQL, both chipping and crack are decreased, provid-ing advantages for reducing surface cracking and increasing fatigue life.

Residual stress

The RS is measured by X-Ray Diffraction (Bruker, D8), using the sin2c method and

the Mn target. Five measuring points are taken on each plan and then take the average. The electrolyte is mixed with CH3OH (90%) and HClO4 (10%), and the depth of each elec- trolysis is 5 mm.

The RS is mainly caused by uneven plastic deforma- tion in cutting. The CRS is usually beneficial, and the TRS is usually harmful, which will reduce structure yield strength. The RS also plays an important role in the working properties of materials, especially fatigue life, crack corrosion, fracture, and wear resistance properties.36 The thermal effect leads to TRS on the surface, while the mechanical effect leads to CRS.37 The varia- tion of the RS with depth is shown in Figure 10(a). It is

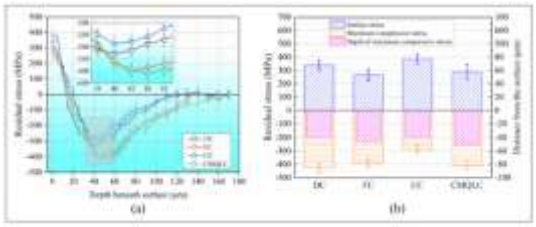

Figure 10. Residual stress under different CL conditions: (a) variation trend and (b) stress characterization.

observed that the surface stress is always TRS, and it of FC and CMQLC is lower; the RS in the subsurface is mainly CRS, which is the result of the increase of mechanical load and plastic deformation flow. At around 20 mm depth, the TRS changes into CRS, and CRS grows at a fast rate as depth increases. At 40, 45, 40, and 50 mm below the surface, respectively, DC, FC, CC, and CMQLC achieve the maximum compressive residual stress (MCRS). Although CC, CMQLC, and FC all attain CRSs, DC's is the biggest.

Its anti-fatigue performance is best when Ra is small and CRS ampli-tude value is large. With a CRS amplitude value of 2409.43 MPa and the lowest Ra of any material, CMQL stands out. This is a great method for ensuring that your material will not wear out quickly. Furthermore, as a reference for characterising with excellent TRS, the surface TRS decreases with increasing MCRS and positioning depth (Figure 10(b)). The aforementioned characterisation reference is supposed to be represented by a weight parameter l, which is determined by formula (1). Versions 1.68, 1.75, 1.10, and 2.02 are the four CL techniques. The RS's ability to prolong component life is directly proportional to the size of l.

$$\lambda = (Rs_{\max\_compressive} \cdot Depth - Rs_{surface}) \cdot 10^{-4} \quad (1)$$

where Rsmax compressive is the MCRS, MPa; Depth is the depth of MCRS, mm; Rssurface is the RS on the surface, MPa.

On the other hand, cutting force and temperature influence surface RS.38 The force-heat ratio e is calcu- lated by Formula (2), and the e is respectively to DC (0.662), FC (2.650), CC (1.339), and CMQLC (1.617).

It is observed that a high e is beneficial to reducing TRS, and has a bigger CRS and depth. It should be noted that although FC has the highest e, it is associ- ated with increased coolant costs and environmental problems. Whereas, for the case of high temperature caused by severe tool wear under cryogenic conditions, TRS may increase accordingly, and the increasing rate of CRS is high with depth increasing, which is the same as the results obtained in Bagherzadeh et al.7 It can be assumed that the cutting conditions with a higher e are effective in extending the fatigue life of the workpiece.22

$$\varepsilon = \frac{\sum F_1 + F_2 + \ldots + F_n}{nT} \quad (2)$$

Where F1–Fn is the average cutting force of n mea- suring areas, N; t is the average cutting temperature, °C. By considering the effect of residual stress on fatigue life, the cost of coolant, and environmental protection, CMQL is the optimized CL condition for cutting Inconel 718 superalloy.

4. CONCLUSION

In order to enhance the efficiency of machining and the longevity of Inconel 718 parts, this study compares and analyses the material's cutting performance and surface integrity in four CL modes: DC, FC, CC, and CMQLC. The following are the primary findings:

(1) Among the three methods, the CMQLC offers the most effective cutting performance in the long run. Cutting forces that are both lower and more consistent may be accomplished with the help of CMQLC. Compared to DC, the average cutting temperature is 55.47 degrees lower. The compact, smooth surface allows for efficient discharging of the short, non-serrated chips. There has been a 25% decrease from FC, and the tool is now the area with the least chipping.

When cutting Inconel 718, the CMQL achieves a surface integrity that is second to none. The FC value is 32.05 percent higher than the lowest Ra that was achieved under the CMQL condition. While the PDL is around thirteen millimetres deep, the white layer is just half that thick. While FC's TRS is 7.9% bigger than CMQLC's, the former has a higher subsurface MCRS and a greater impact depth, increasing by 3.9% and 10.2%, respectively. Increasing the force-heat ratio during cutting may enhance RS both underneath and on the surface, which in turn can lengthen the fatigue life.

(3) The coolant's cooling function is enhanced since the FC dissipates a significant amount of heat. With CMQL's oil mist lubrication, the surface clings to microscopic chips, leaving behind microscopic scratches. Although it has the finest surface polish, it somewhat alters the overall surface roughness. The lack of lubrication caused by cryogenic gas during pre-cooling led to significant wear and chipping of the tool. Therefore, it is incorrect to cool high-hardness materials without first applying lubricant.

(4) Research on cutting performance and surface integrity has shown that CMQL offers the highest overall performance when cutting Inconel 718. A better CRS dispersion, longer tool life, less coolant consumption, and a smoother surface are some of its advantages.

REFERENCES

1. Mia M, Rahman MA, Gupta MK, et al. Advanced cooling-lubrication technologies in metal machining. In: Pramanik A (ed.) Machining and tribology. Amsterdam: Elsevier, 2022, pp.67–92.
2. Anand N, Kumar AS and Paul S. Effect of cutting fluids applied in MQCL mode on machinability of Ti-6Al-4V. J Manuf Process 2019; 43: 154–163.
3. Arunachalam RM, Mannan MA and Spowage AC. Residual stress and surface roughness when facing age hardened Inconel 718 with CBN and ceramic cutting tools. Int J Mach Tools Manuf 2004; 44: 879–887.
4. Pusavec F, Hamdi H, Kopac J, et al. Surface integrity in cryogenic machining of nickel based alloy—Inconel 718. J Mater Process Technol 2011; 211: 773–783.
5. Holmberg J, Wretland A, Hammersberg P, et al. Surface integrity investigations for prediction of fatigue proper- ties after machining of alloy 718. Int J Fatigue 2021; 144: 106059.
6. Sharma VS, Dogra M and Suri NM. Cooling techniques for improved productivity in turning. Int J Mach Tools Manuf 2009; 49: 435–453.
7. Bagherzadeh A, Kuram E and Budak E. Experimental evaluation of eco-friendly hybrid cooling methods in slot milling of titanium alloy. J Clean Prod 2021; 289: 125817.
8. Szczotkarz N, Mrugalski R, Maruda RW, et al. Cutting tool wear in turning 316L stainless steel in the conditions of minimized lubrication. Tribol Int 2021; 156: 106813.

9. Maruda RW, Krolczyk GM, Feldshtein E, et al. Tool wear characterizations in finish turning of AISI 1045 car- bon steel for MQCL conditions. Wear 2017; 372–373: 54–67.
10. Pereira O, Martı´n-Alfonso JE, Rodrı´guez A, et al. Sus- tainability analysis of lubricant oils for minimum quantity lubrication based on their tribo-rheological performance. J Clean Prod 2017; 164: 1419–1429.
11. Chen J, Yu W, Zuo Z, et al. Tribological properties and tool wear in milling of in-situ TiB2/7075 Al composite under various cryogenic MQL conditions. Tribol Int 2021; 160: 107021.
12. Maruda RW, Krolczyk GM, Nies1ony P, et al. Chip for- mation zone analysis during the turning of austenitic stainless steel 316L under MQCL cooling condition. Pro- cedia Eng 2016; 149: 297–304.
13. Naskar A, Singh BB, Choudhary A, et al. Effect of differ- ent grinding fluids applied in minimum quantity cooling- lubrication mode on surface integrity in cBN grinding of Inconel 718. J Manuf Process 2018; 36: 44–50.
14. Ostrowicki N, Kaim A, Gross D, et al. Effect of various cooling lubricant strategies on turning Inconel 718 with different cutting materials. Procedia CIRP 2021; 101: 350–353.
15. Gupta MK, Mia M, Pruncu CI, et al. Parametric optimi- zation and process capability analysis for machining of nickel-based superalloy. Int J Adv Manuf Technol 2019; 102: 3995–4009.
16. Marques A, Paipa Suarez M, Falco Sales W, et al. Turn- ing of Inconel 718 with whisker-reinforced ceramic tools applying vegetable-based cutting fluid mixed with solid lubricants by MQL. J Mater Process Technol 2019; 266: 530–543.
17. Pereira O, Catala` P, Rodrı´guez A, et al. The use of hybrid CO2 + MQL in machining operations. Procedia Eng 2015; 132: 492–499.
18. Polvorosa R, Sua´rez A, de Lacalle LNL, et al. Tool wear on nickel alloys with different coolant pressures: compar- ison of Alloy 718 and Waspaloy. J Manuf Process 2017; 26: 44–56.
19. Pereira O, Celaya A, Urbikaı´n G, et al. CO2 cryogenic milling of Inconel 718: cutting forces and tool wear. J Mater Res Technol 2020; 9: 8459–8468.
20. Pereira O, Urbikain G, Rodrı´guez A, et al. Internal cryo- lubrication approach for Inconel 718 milling. Procedia Manuf 2017; 13: 89–93.
21. Boozarpoor M, Teimouri R and Yazdani K. Compre- hensive study on effect of orthogonal turn-milling para- meters on surface integrity of Inconel 718 considering production rate as constrain. Int J Lightweight Mater Manuf 2021; 4: 145–155.
22. Jiang X, Kong X, He S, et al. Modeling the superposition of residual stresses induced by cutting force and heat dur- ing the milling of thin-walled parts. J Manuf Process 2021; 68: 356–370.
23. Vovk A, So¨lter J and Karpuschewski B. Finite element simulations of the material loads and residual stresses in milling utilizing the CEL method. Procedia CIRP 2020; 87: 539–544.
24. Jeyapandiarajan P and Anthony XM. Evaluating the machinability of Inconel 718 under different machining conditions. Procedia Manuf 2019; 30: 253–260.
25. De Bartolomeis A, Newman ST, Jawahir IS, et al. Future research directions in the machining of Inconel 718. J Mater Process Technol 2021; 297: 117260.